



## Review

Carbon properties and their role in supercapacitors<sup>☆</sup>

A.G. Pandolfo\*, A.F. Hollenkamp

CSIRO Division of Energy Technology, Box 312, Clayton South, Vic. 3169, Australia

Available online 4 April 2006

**Abstract**

Supercapacitors (also known as ‘ultracapacitors’) offer a promising alternative approach to meeting the increasing power demands of energy-storage systems in general, and of portable (digital) electronic devices in particular. Supercapacitors are able to store and deliver energy at relatively high rates (beyond those accessible with batteries) because the mechanism of energy storage is simple charge-separation (as in conventional capacitors). The vast increases in capacitance achieved by supercapacitors are due to the combination of: (i) an extremely small distance that separates the opposite charges, as defined by the electric double-layer; (ii) highly porous electrodes that embody very high surface-area. A variety of porous forms of carbon are currently preferred as the electrode materials because they have exceptionally high surface areas, relatively high electronic conductivity, and acceptable cost. The power and energy-storage capabilities of these devices are closely linked to the physical and chemical characteristics of the carbon electrodes. For example, increases in specific surface-area, obtained through activation of the carbon, generally lead to increased capacitance. Since only the electrolyte-wetted surface-area contributes to capacitance, the carbon processing is required to generate predominantly ‘open’ pores that are connected to the bulk pore network. While the supercapacitors available today perform well, it is generally agreed that there is considerable scope for improvement (e.g., improved performance at higher frequencies). Thus it is likely that carbon will continue to play a principal role in supercapacitor technology, mainly through further optimization of porosity, surface treatments to promote wettability, and reduced inter-particle contact resistance.

© 2006 Published by Elsevier B.V.

**Keywords:** Supercapacitor; Ultracapacitor; Porosity; surface-area; Activated carbon; Capacitance**Contents**

1. Introduction .....	12
2. Energy storage in electrochemical double-layer capacitors .....	13
3. EDLC construction .....	13
4. Electrode material characteristics .....	14
4.1. Carbon structure and form .....	14
4.1.1. Engineered carbons .....	15
4.1.2. Activation .....	16
4.1.3. Electrical properties .....	16
4.1.4. Carbon surface functionalities .....	18
4.1.5. Double-layer capacitance of carbon materials .....	19
4.2. Carbon surface-area and porosity .....	20
4.3. Carbon forms .....	21
4.3.1. Carbon blacks .....	22
4.3.2. Carbon aerogels .....	22
4.3.3. Carbon fibres .....	22
4.3.4. Glassy carbons .....	23

\* Corresponding author.

E-mail address: [tony.pandolfo@csiro.au](mailto:tony.pandolfo@csiro.au) (A.G. Pandolfo).<sup>☆</sup> This review is one of a series dealing with the role of carbon in electrochemical energy storage. The review covering the role of carbon in valve-regulated lead-acid battery technology is also published in this issue, *J. Power Sources*, volume 157, issue 1, pages 3–10. The reviews covering the role of carbon in fuel cells and the role of carbon in graphite and carbon powders were published in *J. Power Sources*, volume 156, issue 2, pages 128–150.

4.4. Carbon nanostructures .....	23
5. Summary .....	24
Acknowledgements .....	25
References .....	25

## 1. Introduction

Supercapacitors, ultracapacitors and electrochemical double-layer capacitors (EDLCs) are commonly used names for a class of electrochemical energy-storage devices that are ideally suited to the rapid storage and release of energy. The term ‘supercapacitor’ is adopted in this paper. Compared with conventional capacitors, the specific energy of supercapacitors is several orders of magnitude higher (hence the ‘super’ or ‘ultra’ prefix). Supercapacitors also have a higher specific power than most batteries, but their specific energy is somewhat lower. Through appropriate cell design, both the specific energy and specific power ranges for supercapacitors can cover several orders of magnitude and this makes them extremely versatile as a stand-alone energy supply, or in combination with batteries as a hybrid system. This unique combination of high power capability and good specific energy, allows supercapacitors to occupy a functional position between batteries and conventional capacitors (Fig. 1 and Table 1).

Supercapacitors are particularly useful because their parameters complement the deficiencies of other power sources such as batteries and fuel cells. Due to their highly reversible charge-storage process, supercapacitors have longer cycle-lives and can be both rapidly charged and discharged at power densities exceeding  $1 \text{ kW kg}^{-1}$  [1]. These features have generated great interest in the application of supercapacitors for a wide, and growing, range of applications that include: consumer electronics, hybrid electric vehicles, and industrial power management [2–4].

Research into supercapacitors is presently divided into two main areas that are based primarily on their mode of energy storage, namely: (i) the redox supercapacitor and (ii) the electrochemical double layer capacitor.

In redox supercapacitors (also referred to as pseudocapacitors), a reversible Faradaic-type charge transfer occurs and the resulting capacitance, while often large, is not electrostatic in origin (hence the ‘pseudo’ prefix to provide differentiation from electrostatic capacitance). Rather, capacitance is associated with an electrochemical charge-transfer process that takes place to an extent limited by a finite amount of active material or available surface [5]. The most commonly investigated classes of pseudocapacitive materials are transition metal oxides (notably, ruthenium oxide) and conducting polymers such as polyaniline, polypyrrole or derivatives of polythiophene [6–9]. Given that charge storage is based on a redox process, this type of supercapacitor is somewhat battery-like in its behaviour.

By comparison, the EDLC stores energy in much the same way as a traditional capacitor, by means of charge separation. Supercapacitors can, however, store substantially more energy (per unit mass or volume) than a conventional capacitor (by several orders of magnitude) because: (i) charge separation takes place across a very small distance in the electrical double-layer that constitutes the interphase between an electrode and the adjacent electrolyte [5]; (ii) an increased amount of charge can be stored on the highly extended electrode surface-area (created by a large number of pores within a high surface-area electrode material). The mechanism of energy storage is inherently rapid because it simply involves movement of ions to and from electrode surfaces. In batteries, additional steps, such as heterogeneous charge-transfer and chemical phase changes, introduce relatively slow steps into the process of energy storage and delivery. For similar reasons, EDLCs exhibit a very high degree of reversibility in repetitive charge–discharge cycling—demonstrated cycle lives in excess of 500,000 cycles have been achieved [10].

A number of reviews have discussed the science and technology of supercapacitors for various configurations and electrode materials [5,11–13]. The EDLC version of the supercapacitor is the most developed form of electrochemical capacitor. Carbon, in its various forms, is currently the most extensively examined and widely utilised electrode material in EDLCs with development focusing on achieving high surface-area with low matrix resistivity. A number of carbon manufacturers are now targeting supercapacitors as a market for their products [14,15].

Carbon materials have long been incorporated into the electrodes of energy-storage devices as: electro-conductive additives, supports for active materials, electron transfer catalysts, intercalation hosts, substrates for current leads, and as agents for the control of heat transfer, porosity, surface-area and capacitance [16]. For these reasons, carbons are of course also well suited as electrode materials for EDLCs.

It is clear that the ultimate performance of carbon-based supercapacitors will be closely linked to the physical and chemi-

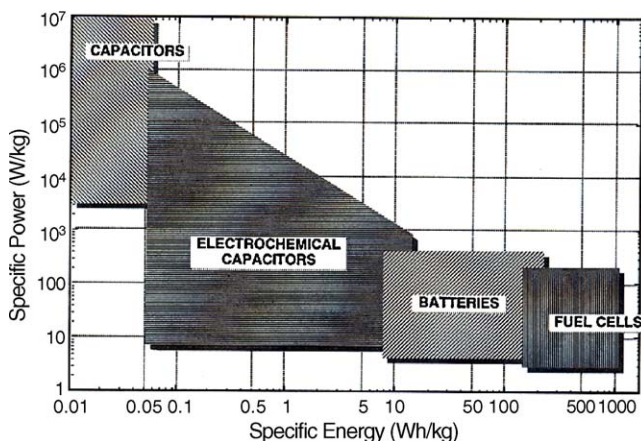


Fig. 1. Specific energy and power capabilities of capacitors (electrostatic), electrochemical capacitors (supercapacitors), batteries and fuel cells [13].

Table 1  
Comparison of typical capacitor and battery characteristics (adapted from Ref. [36])

Characteristic	Electrolytic capacitor	Carbon supercapacitor	Battery
Specific energy (Wh kg <sup>-1</sup> )	<0.1	1–10	10–100
Specific power (W kg <sup>-1</sup> )	≥10000	500–10000	<1000
Discharge time	10 <sup>-6</sup> to 10 <sup>-3</sup> s	s to min	0.3–3 h
Charging time	10 <sup>-6</sup> to 10 <sup>-3</sup> s	s to min	1–5 h
Charge/discharge efficiency (%)	~100	85–98	70–85
Cycle-life (cycles)	Infinite	>500000	~1000
Max. voltage (V <sub>max</sub> ) determinants	Dielectric thickness and strength	Electrode and electrolyte stability window	Thermodynamics of phase reactions
Charge stored determinants	Electrode area and dielectric	Electrode microstructure and electrolyte	Active mass and thermodynamics

cal characteristics of the carbon electrodes. Due to the enormous range of carbon materials that are available, an understanding of carbon materials and their properties is desirable for matching carbon characteristics with supercapacitor applications. In this study, we describe the role of carbon in EDLCs and discuss the implications of carbon structure on the physical and chemical properties of these devices.

## 2. Energy storage in electrochemical double-layer capacitors

The concept of the double layer has been studied by chemists since the 19th century when von Helmholtz first developed and modelled the double layer concept in investigations on colloidal suspensions [17]. This work was subsequently extended to the surface of metal electrodes in the late 19th and early-mid-20th centuries [18–22]. In 1957, the practical use of a double-layer capacitor, for the storage of electrical charge, was demonstrated and patented by General Electric [23]. This early patent utilised crude porous carbon electrodes in an aqueous electrolyte. Not until the granting of a patent to SOHIO in 1966 [24] was it acknowledged that these devices actually store energy in the electrical double-layer, at the interphase between electrode and solution. The first commercial double-layer supercapacitors originated from SOHIO [25] who went on to patent a disc-shaped device that consisted of carbon paste electrodes, formed by soaking porous carbon in an electrolyte separated by an ion-permeable separator [26]. SOHIO also utilized non-aqueous electrolytes in their early devices, but, a lack of sales

saw them license their technology to NEC in 1971; who further developed and successfully marketed double-layer supercapacitors, primarily for memory backup applications [27]. These early devices typically had a low voltage and a high internal resistance [28].

By the 1980s a number of companies were producing double-layer capacitors, e.g., Matsushita (Gold capacitor), Elna (Dynacap) and PRI (PRI ultracapacitor), although the last-mentioned incorporated relatively expensive metal oxide electrodes, primarily targeted for military applications. Today, a number of high-performance EDLC devices, based on porous carbons, are commercially available from a range of manufacturers and distributors around the world (Table 2, [29]).

## 3. EDLC construction

Supercapacitors are constructed much like a battery in that there are two electrodes immersed in an electrolyte, with an ion permeable separator located between the electrodes (Fig. 2). In such a device, each electrode–electrolyte interface represents a capacitor so that the complete cell can be considered as two capacitors in series. For a symmetrical capacitor (similar electrodes), the cell capacitance ( $C_{\text{cell}}$ ), will therefore be

$$\frac{1}{C_{\text{cell}}} = \frac{1}{C_1} + \frac{1}{C_2} \quad (1)$$

where  $C_1$  and  $C_2$  represent the capacitance of the first and second electrodes, respectively [10]. (Note: literature values of specific capacitance often quote the capacitance of a single carbon elec-

Table 2  
Commercially available EDLCs<sup>a</sup>

Company name	Device name	Capacitance (F)	Cell/module voltage (V)	Type
Asahi Glass	EDLC	500–2000	3, 14/42	Carbon/non-aqueous
AVX	Bestcap	0.022–0.56	3.5–12	Carbon/polymer/aqueous
Cap-XX	Supercapacitor	0.09–2.8	2.25–4.5	Carbon/non-aqueous
Cooper	PowerStor	0.47–50	2.3–5	Aerogel/non-aqueous
ELNA	Dynacap	0.333–100	2.5–6.3	Carbon/non-aqueous
Epcos	Ultracapacitor	5–5000	2.3, 2.5	Carbon/non-aqueous
Evans	Capattery	0.01–1.5	5.5, 11	Carbon/aqueous
Maxwell	Boostcap/PowerCache	1.8–2600	2.5	Carbon/non-aqueous
NEC	Supercapacitor	0.01–6.5	3.5–12	Carbon/aqueous Carbon/organic
Nippon Chemi-Con	DLCAP	300–3000	2.3, 2.5	Carbon/non-aqueous
Ness	NessCap	3–5000	2.3, 2.7	Carbon/organic
Matsushita/Panasonic	Gold capacitor	0.1–2500	2.3–5.5	Carbon/organic
Tavrira/ECOND	Supercapacitor	0.13–160	14–300	Carbon/aqueous

<sup>a</sup> Information derived from company web-sites and does not represent an exhaustive listing of all available suppliers or devices (adapted from Ref. [29]).

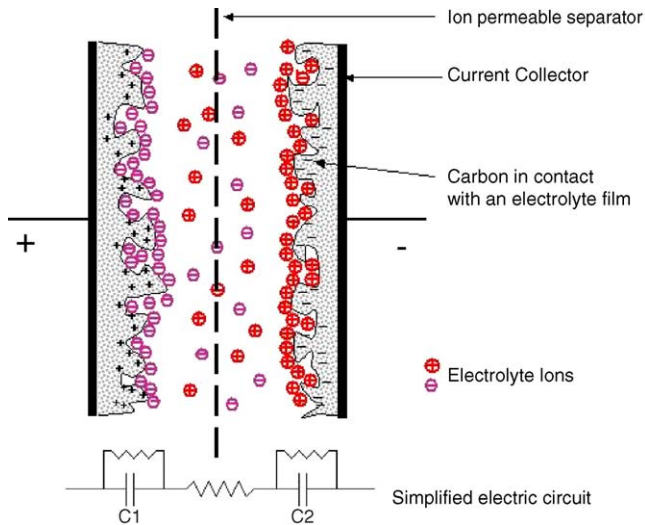


Fig. 2. Representation of an electrochemical double layer capacitor (in its charged state).

trode, usually derived from a three-electrode laboratory test cell that also incorporates a reference and counter electrode [30].)

The double layer capacitance,  $C_{dl}$ , at each electrode interface is given by

$$C_{dl} = \frac{\varepsilon A}{4\pi t} \quad (2)$$

where  $\varepsilon$  is the dielectric constant of the electrical double-layer region,  $A$  the surface-area of the electrode and  $t$  is the thickness of the electrical double layer. In double-layer capacitors, it is the combination of high surface-area (typically  $>1500 \text{ m}^2 \text{ g}^{-1}$ ) with extremely small charge separation (Angstroms) that is responsible for their extremely high capacitance [31]. The energy ( $E$ ) and power ( $P_{\max}$ ) of supercapacitors are calculated according to

$$E = \frac{1}{2} CV^2 \quad (3)$$

$$P_{\max} = \frac{V^2}{4R} \quad (4)$$

where  $C$  is the dc capacitance in Farads,  $V$  the nominal voltage, and  $R$  is the equivalent series resistance (ESR) in ohms [10].

The capacitance of a device is largely dependent on the characteristics of the electrode material; particularly, the surface-area and the pore-size distribution. Due to the high porosity, and correspondingly low density of carbons, it is usually the volumetric capacitance of each electrode that determines the energy density [32].

Cell voltage is also an important determinant of both the specific energy and the power of supercapacitors. The operating voltage of supercapacitors is usually dependant on electrolyte stability. Aqueous electrolytes, such as acids (e.g.,  $\text{H}_2\text{SO}_4$ ) and alkalis (e.g.,  $\text{KOH}$ ) have the advantage of high ionic conductivity (up to  $\sim 1 \text{ S cm}^{-1}$ ), low cost and wide acceptance. On the other hand, they have the inherent disadvantage of a restricted voltage range with a relatively low decomposition voltage of  $\sim 1.23 \text{ V}$  [33]. Nevertheless, the specific capacitance ( $\text{Farads g}^{-1}$ ) of high surface-area carbons in aqueous electrolytes tends to be signif-

icantly higher than that of the same electrode in non-aqueous solutions owing to the higher dielectric constant that pertains to aqueous systems [34].

Non-aqueous electrolytes of various types have been developed that allow the use of cell operating voltages above  $2.5 \text{ V}$  [33,35]. Since the specific energy of supercapacitors is proportional to the square of the operating voltage, non-aqueous electrolyte mixtures such as propylene carbonate or acetonitrile, containing dissolved quaternary alkyl ammonium salts, have been employed in many commercial supercapacitors, particularly those targeting higher energy applications. The electrical resistivity of non-aqueous electrolytes is, however, at least an order of magnitude higher than that of aqueous electrolytes and therefore the resulting capacitors generally have a higher internal resistance.

A high internal resistance limits the power capability of the capacitor and, ultimately, its application. In supercapacitors, a number of sources contribute to the internal resistance and are collectively measured and referred to as the equivalent series resistance, or ESR [10,36]. Contributors to the ESR of supercapacitors include:

- electronic resistance of the electrode material;
- the interfacial resistance between the electrode and the current-collector;
- the ionic (diffusion) resistance of ions moving in small pores;
- the ionic resistance of ions moving through the separator;
- the electrolyte resistance.

#### 4. Electrode material characteristics

The attraction of carbon as a supercapacitor electrode material arises from a unique combination of chemical and physical properties, namely:

- high conductivity,
- high surface-area range ( $\sim 1$  to  $>2000 \text{ m}^2 \text{ g}^{-1}$ ),
- good corrosion resistance,
- high temperature stability,
- controlled pore structure,
- processability and compatibility in composite materials,
- relatively low cost.

In general terms, the first two of these properties are critical to the construction of supercapacitor electrodes. As will be seen, the properties of carbon allow both conductivity and surface-area to be manipulated and optimised. Such activities continue to be the subject of a considerable amount of research. Prior to reviewing the results of this research, it is useful first to consider in more detail other aspects of carbon, e.g., its structural diversity and chemical behaviour, so as to establish a better understanding of the role of carbon materials in supercapacitors.

##### 4.1. Carbon structure and form

Carbon has four crystalline (ordered) allotropes: diamond ( $\text{sp}^3$  bonding), graphite ( $\text{sp}^2$ ), carbyne ( $\text{sp}^1$ ) and fullerenes ('dis-

torted'  $sp^2$ ). While two carbon allotropes are naturally found on earth as minerals, namely, natural graphite and diamond, the other forms of carbon are synthetic. Carbon is considered unusual in the number of its allotropic structures and the diversity of structural forms, as well as in its broad range of physical properties [37,38].

Due to the wide range of carbon materials, and to avoid confusion, the term 'carbon' is typically used to describe the element rather than its form. To describe a carbon-based material, it is best coupled with a qualifier such as 'carbon black', 'activated carbon', 'vitreous carbon' and others. A comprehensive guide to the terminology and description of carbon solids, as used in the science and technology of carbon and graphite materials, is available [39].

#### 4.1.1. Engineered carbons

The majority of commercial carbons used today can be conveniently described as 'engineered carbons'. These are manufactured carbons that have an amorphous structure with a more or less disordered microstructure based on that of graphite [37]. Amorphous carbons can be considered as sections of hexagonal carbon layers with very little order parallel to the layers. The process of graphitisation consists essentially of the ordering and stacking of these layers and is generally achieved by high-temperature treatment ( $>2500^\circ\text{C}$ ). Between the extremes of amorphous carbon and graphite, a wide variety of carbon materials can be prepared and their properties tailored, to some extent, for specific applications.

The majority of carbon materials are derived from carbon-rich organic precursors by heat treatment in inert atmospheres (a process referred to as carbonization). The ultimate properties of these carbons are dependent on a number of critical factors, e.g., the carbon precursor, its dominant aggregation state during carbonization (i.e., gas, liquid or solid), processing conditions, and the structural and textural features of the products [40].

Summaries of the key processing conditions that lead to specific carbon products (and their features) are outlined in Table 3.

During carbonization, carbon precursors go through a thermal decomposition (pyrolysis), which eliminates volatile materials that include heteroatoms. With increasing temperature, condensation reactions are initiated and localized graphitic units commence to grow and become aligned into small 'graphite like' microcrystallites, i.e., stacks of aromatic layers or 'graphene sheets' [41]. The carbon precursor and its processing conditions will determine the size of the graphene sheets ( $L_a$ ), the stacking number of graphene sheets ( $L_c$ ) and the relative orientation of the crystallites. The size and orientation of the crystallites are very important as they define the materials' texture and the degree of electrical conductivity [42].

Some carbon precursors (e.g., petroleum pitch, coal pitch, some polymers) pass through a fluid stage (referred to as mesophase) during carbonization that allows large aromatic molecules to align with each other and form a more extensive pre-graphitic structure. Upon further high-temperature treatment ( $>2500^\circ\text{C}$ ), these carbons can be converted into highly ordered graphite and are referred to as graphitising carbons [41].

Other carbon precursors retain a solid phase during carbonization, and the limited mobility of the crystallites leads to the formation of a rigid amorphous structure that consist of randomly-oriented graphene layers [40]. These materials cannot be readily converted to graphite by further high-temperature treatment and are referred to as non-graphitizing carbons. Non-graphitizing carbons are produced from materials such as biomass (e.g., wood, nut shells, etc.), non-fusing coals and many thermosetting polymers (e.g., polyvinylidene chloride, PVDC). The loss of volatiles and the retention of a rigid and complex molecular structure during the carbonization of many non-graphitizable carbons can lead to a highly porous structure without the need for further activation.

Table 3

Common precursors and controlling production factors for various classes of carbon materials (adapted from Ref. [40])

Carbon material (phase during aggregation)	Common precursors	Controlling production factor	Structural/textural feature
<b>Gas phase</b>			
Carbon blacks	Hydrocarbon gas or liquid	Precursor concentration	Colloidal/nanosized
Pyrolytic carbon	Hydrocarbon gas	Deposition on a substrate	Preferred orientation
Vapour-grown carbon fibres	Hydrocarbon gas	Presence of a catalyst	Catalyst particle size/shape
Fullerene	Graphite rod	Condensation of carbon vapour	Nanosize molecule
Nanotubes	Hydrocarbon vapour	Condensation of carbon vapour	Single wall, multi-wall, chiral
<b>Liquid phase</b>			
Cokes	Coals, petroleum pitch	Shear stress	Mesophase formation and growth
Graphite	Petroleum coke	High temperature	Mesophase formation and growth
Carbon fibres (pitch derived)	Coal pitch, petroleum pitch	Spinning	Mesophase formation and growth
<b>Solid phase</b>			
Activated carbons	Biomass, coals, petroleum coke, selected polymers	Carbonization/activation	Nanosize pores
Molecular sieve carbon	Selected biomass, coals, polymers	Selective pore development	Nanosize pore/constrictions
Glass-like carbons	Thermosetting polymers (e.g., polyfurfuryl alcohol)	Slow carbonization	Random crystallites, impervious
Carbon fibres (polymer derived)	Selected polymers (e.g., polyacrylonitrile)	Slow carbonization	Random crystallites, non-porous
Highly oriented graphite	Pyrolytic carbon, poly-imide film	High molecular orientation	Highly oriented crystallites

#### 4.1.2. Activation

As noted earlier, one of the great attractions of using carbon as an electrode material is that it can be readily converted into a form that has very high specific surface-area. Generally speaking, the process employed to increase surface-area (and porosity) from a carbonised organic precursor (a ‘char’) is referred to as ‘activation’ and the resulting broad group of materials is referred to as activated carbons. Chars usually have a relatively low porosity and their structure consists of elementary crystallites with a large number of interstices between them. The interstices tend to be filled with ‘disorganized’ carbon residues (tars) that block the pore entrances. Activation opens these pores and can also create additional porosity. Varying the carbon precursor and activation conditions (particularly temperature, time and gaseous environment) allows some control over the resulting porosity, pore-size distribution, and the nature of the internal surfaces. Although carbon manufacturers closely guard their procedures for the activation of commercial carbons, the processes can be placed into two general categories: thermal activation and chemical activation [38,43].

Thermal activation, sometimes referred to as physical activation, entails the modification of a carbon char by controlled gasification, and is usually carried out at temperatures between 700 and 1100 °C in the presence of suitable oxidising gases such as steam, carbon dioxide, air, or mixtures of these gases. During gasification, the oxidising atmosphere greatly increases the pore volume and surface-area of the material through a controlled carbon ‘burn-off’ and the elimination of volatile pyrolysis products. The level of burn-off is, perhaps, the most important factor governing the quality of the activated carbon and is controlled by the temperature and duration of activation. A high degree of activation is achieved by increased burn-off, but the additional activity is accompanied by a decrease in carbon strength, a lower density, reduced yield and pore widening.

Chemical activation is usually carried out at slightly lower temperatures (~400–700 °C) and involves the dehydrating action of certain agents such as phosphoric acid, zinc chloride and potassium hydroxide. Post-activation washing of the carbon is usually required to remove residual reactants as well as any inorganic residue (sometimes referred to as ash) that originates from the carbon precursor or is introduced during activation. Exceptionally high surface-area materials (>2500 m<sup>2</sup> g<sup>-1</sup>) have been prepared with potassium hydroxide activation techniques [44].

#### 4.1.3. Electrical properties

The electrical properties of carbon materials are directly related to their structure. For electrode applications, the resistivity/conductivity of the material is a major concern. This applies both to the intrinsic properties of the carbon and to ‘aggregate’ properties, particularly in the common situation where fine particulate forms of carbon are bound together to form a composite electrode structure (v.i.).

Most carbon precursors are generally good insulators (resistivities >10<sup>12</sup> Ω cm) that contain a high proportion of σ or sp<sup>3</sup> bonded carbon structures. The conductivity of solid carbons is strongly influenced by heat treatment in that it increases

rapidly with heat treatment temperature up to ~700 °C and at a much slower rate for heat treatment above 700 °C [45]. The increasing proportion of conjugated carbon in the sp<sup>2</sup> state during carbonization progressively increases the conductivity of the starting material as electrons associated with π-bonds are delocalized and become available as charge carriers [46]. Electrical conductivity increases as separate conjugated systems also become interconnected to form a conducting network. The temperature range at which the conductivity of solid carbon initially begins to level off (600–700 °C) corresponds to the range in which carbons lose acidic functionalities, primarily by formation of H<sub>2</sub>O and CO<sub>2</sub> [45]. Thus heat treatment increases the conductivity of carbons by altering the degree of structural disorder, which can vary from nearly amorphous carbon to the near perfect crystals of graphite (formed at temperatures >2500 °C).

Consistent with the anisotropic nature of graphite, the electronic resistivity of carbons also varies with their degree of crystallographic orientation [47]. The specific resistivity of graphite crystals in the plane of the aromatic rings (*a*-axis direction) is ~10<sup>-5</sup> Ω cm, whereas perpendicular to this plane, along the *c* axis, the resistivity is in the vicinity of 10<sup>-2</sup> Ω cm [48]. The resistivity of selected representative carbon materials are shown in Fig. 3 and can vary by at least three orders of magnitude, which range from that of semiconductors to semi-metals [49].

Whilst the ‘intrinsic’ (i.e., intra-particle) resistivity of a carbon material is dependent on its chemical and structural morphology, the electrical resistance of a packed bed of carbon particles is a function of both its intra-particle resistance and the contact (or inter-particle) resistance [28,46]. In addition, for a porous carbon artefact, there is a resistance associated with the current-carrying path, through the carbon particle, across the carbon/carbon and carbon/metallic collector interfaces, and through the metallic collector. Although there could be a number of equivalent paths to a particular point, the value of the

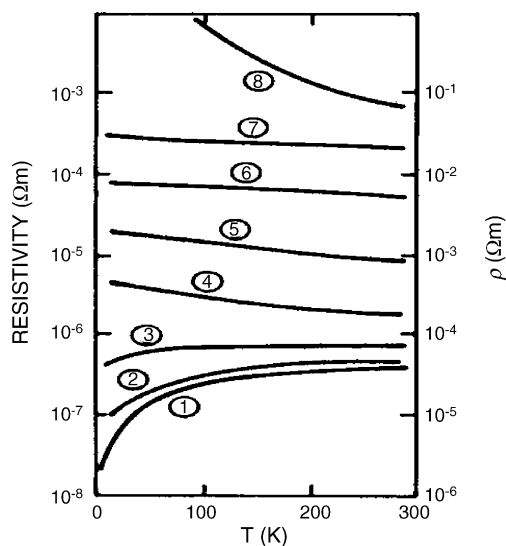


Fig. 3. Resistivity ( $\rho$ ) vs. temperature plots for various forms of carbon: (1) single crystal graphite; (2) highly oriented pyrolytic graphite; (3) graphite whisker; (4) pyrolytic graphite; (5) petroleum coke carbon; (6) lampblack carbon; (7) glassy carbon; (8) carbon film—electron beam evaporated [49].

Table 4  
Resistivities of several types of powdered carbons under differing compaction pressures [50]

Sample	Resistivity ( $\Omega$ cm)		
	200 kgf <sup>a</sup> cm <sup>-2</sup>	1000 kgf <sup>a</sup> cm <sup>-2</sup>	2000 kgf <sup>a</sup> cm <sup>-2</sup>
Electrographite	$1.40 \times 10^{-3}$	$7.70 \times 10^{-3}$	$6.81 \times 10^{-3}$
Active carbon (Riedel de-Haen)	1.07	$2.90 \times 10^{-1}$	$1.79 \times 10^{-1}$
Carbon-black (SRF)	$3.93 \times 10^{-1}$	$6.10 \times 10^{-2}$	$2.44 \times 10^{-2}$
Acetylene-black	$1.78 \times 10^{-1}$	$4.86 \times 10^{-2}$	$2.64 \times 10^{-2}$
Petroleum coke (1400 °C)	$1.50 \times 10^{-1}$	$3.02 \times 10^{-2}$	$1.96 \times 10^{-2}$
Petroleum coke (1600 °C)	$6.47 \times 10^{-2}$	$1.74 \times 10^{-2}$	$1.35 \times 10^{-2}$
Babaçu nut coke	1.24	$2.72 \times 10^{-1}$	$1.21 \times 10^{-1}$
Eucalyptus lignite carbon	$9.21 \times 10^{-1}$	$1.90 \times 10^{-1}$	$9.57 \times 10^{-2}$

<sup>a</sup> Kilogram of force used in original reference work, kgf = 9.8 N.

resistance associated with the path will be a function of: (i) the position within the bed, (ii) packing parameters, and (iii) the resistance of the carbon material itself [28].

Particle contact resistance is a major contributor to the resistance of aggregated carbon powders and is highly dependent on both the physical morphology of the carbon particle (e.g., size, shape, aggregation, etc.) and the pressure that is applied to compact the particles [28,46,50]. Espinola et al. [50], measured the electrical properties of a range of carbon powders as a function of compaction pressure, see Table 4. It was found that greater compaction pressure leads to a decrease in resistivity and that only at high compaction pressures does the measured resistivity of a packed carbon powder begin to approach asymptotically the intrinsic resistivity of the carbon material itself.

Packing pressure compresses the particle bed and produces better contact between particles and reduces the path length through the bed. The effect of pressure is generally larger for smaller particles. A closely-packed structure also minimizes the amount of electrolyte contained in the inter-particle void space formed between the irregular carbon particles, although in supercapacitors this needs to be carefully balanced against electrolyte requirements to avoid electrolyte-depletion effects. One of the advantages of the use of carbon powders is to allow the thickness of the carbon coating to be easily manipulated and this, in turn, enables the preparation of electrodes of varying shapes and capacities. The use of thin coating films (containing small particles of appropriate size) generally results in low ESR electrodes that are well suited to high charge–discharge applications [28].

The presence of surface oxygen also affects the resistivity of carbon powders [46,51]. Oxygen functionalities, which preferentially form at the edges of the graphite like microcrystallites, increase the barrier for electrons to transfer from one microcrystalline element to the next [52,53]. Therefore, processes that increase the surface oxygen content of carbons, for example by the exposure of carbons to oxygen at elevated temperatures or by prolonged grinding, also increase their electrical resistivity. Conversely, the removal of surface oxides, by heat treatment (at  $\sim 1000$  °C) in an inert atmosphere, decreases the electrical resistivity of carbon powders [48].

In preparing electrodes based on powdered activated carbons, it is standard practice to employ an organic (usually polymeric) binding agent to establish and maintain an electrode structure. Here, with the maintenance of maximum conductivity in mind, it

is essential that the binder be well distributed and used sparingly to avoid the formation of an electrically insulating layer between the carbon particles. Excessive amounts of binder will increase the electrode resistance, largely through a greater particle contact resistance, and will ultimately contribute to an increase in the capacitor ESR [54].

There are varying reports in the literature on the effect of increasing surface-area and porosity on the intrinsic electronic conductivity of compacted carbon powders. Intuitively, it would be expected that the volumetric conductivity decreases as the porosity and surface-area increase (for carbons experiencing similar treatment temperatures) since the number of conductive pathways would also be expected to decrease. Generally, this trend is infrequently observed, but is more noticeable when comparing similar carbon materials [51,55]. The most likely explanation is that carbons with a similar surface-area or porosity do not necessarily have the same physical, or even chemical, structure. As outlined earlier, variations in carbon precursor, thermal treatment, the presence (or absence) of surface functionalities and associated changes in the mode of electronic conduction [46], are more likely to influence the resistivity of compacted carbon powders than variations in surface-area or porosity alone. It should also be acknowledged that the electrical resistance of the carbon material is one of several possible contributors to the capacitor ESR [10,28]. Whilst the carbon (intrinsic) electrical resistance needs to be kept to a minimum the capacitor ESR may ultimately be governed by other, more dominant ESR contributors that can sometimes overshadow minor contributors.

An important factor in determining capacitor ESR is the attachment of the carbon material to the metallic current-collector. The interfacial electrical resistance between the carbon and collector can be a major contributor to capacitor ESR and long-term stability. It is influenced by factors such as carbon morphology, particle size, surface functionalities, cleanliness of the metallic substrate (i.e., free from surface impurities), the presence of a binder, electrode form/shape, electrolyte, and cell design (especially containment pressure). Even with the use of binders, it is challenging to adhere carbons to metallic surfaces in a manner that does not substantially increase capacitor ESR and maintains stability over the lifetime of the capacitor. Various chemical and physical treatments are often applied to metallic substrates in order to improve carbon-binder adhesion and stabi-

lize the carbon/metal interface [56]. The use of highly etched or even porous metallic substrates (e.g., metal gauze, metal foams) also assists carbon adhesion by physically locking, or ‘keying in’, the carbon to the porous metal collector, and by providing an increase in contact surface-area [54,57].

#### 4.1.4. Carbon surface functionalities

For carbon-based double-layer capacitors, the presence of surface groups is known to influence the electrochemical interfacial state of the carbon surface and its double-layer properties that include: wettability, point of zero charge, electrical contact resistance, adsorption of ions (capacitance), and self-discharge characteristics [5,58]. Graphitic carbon surfaces can be regarded as being made up of (at least) two chemically different kinds of sites: basal and edge carbon sites [45]. Edge sites are considered to be more reactive than basal sites as they are often associated with unpaired electrons. This view is supported by the observation that the reactivity of edge sites towards oxygen, for high purity graphite, is an order of magnitude greater than that of basal sites [45]. Consequently, the chemical properties of carbons also vary with the relative fraction of edge sites and basal plane sites; with the ratio of edge to basal sites generally increasing with the degree of disorder.

Porous carbons are almost invariably associated with appreciable concentrations of heteroatoms, which are primarily oxygen and hydrogen, and to a lesser degree, nitrogen, sulfur and halogens [43,48]. These heteroatoms are derived from the starting materials and become part of the chemical structure as a result of incomplete carbonization. They may also be incorporated on to the carbon surface during subsequent treatment or exposure to air. Carbons can readily physisorb (i.e., reversible adsorption) molecular oxygen upon exposure to air, even at sub-ambient temperatures [49]. Oxygen chemisorption (irreversible adsorption) also begins to occur at low temperatures (e.g., ambient) and increases with temperature to form various oxygen-based functionalities on the carbon surface [48,59]. Carbon–oxygen complexes are by far the most important surface group on carbons.

Three types of surface oxides, namely, acidic, basic and neutral, have been proposed to form on carbon surfaces as determined by the formation history of the carbon material and the temperature at which it was first exposed to oxygen [46,60]. Acidic surface oxides are formed when carbons are exposed to oxygen between 200 and 700 °C or by reactions with oxidizing solutions at room temperature. These surface groups are considered to be less stable and include groups such as carboxylic, lactonic and phenolic functionalities. Basic and neutral surface oxides are considered to be more stable than acidic oxides and tend to form after a carbon surface, freed from all surface compounds by heat treatment, comes in contact with oxygen at low temperatures [46,60]. Functional groups that are electrochemically inert in the potential range of operation can enhance the wettability of carbon electrodes and, consequently, increase the specific capacitance of the carbon through improved pore access and greater surface utilization [61].

The extent of oxygen retention as physically adsorbed molecular oxygen, or as surface complexes, is believed to influence

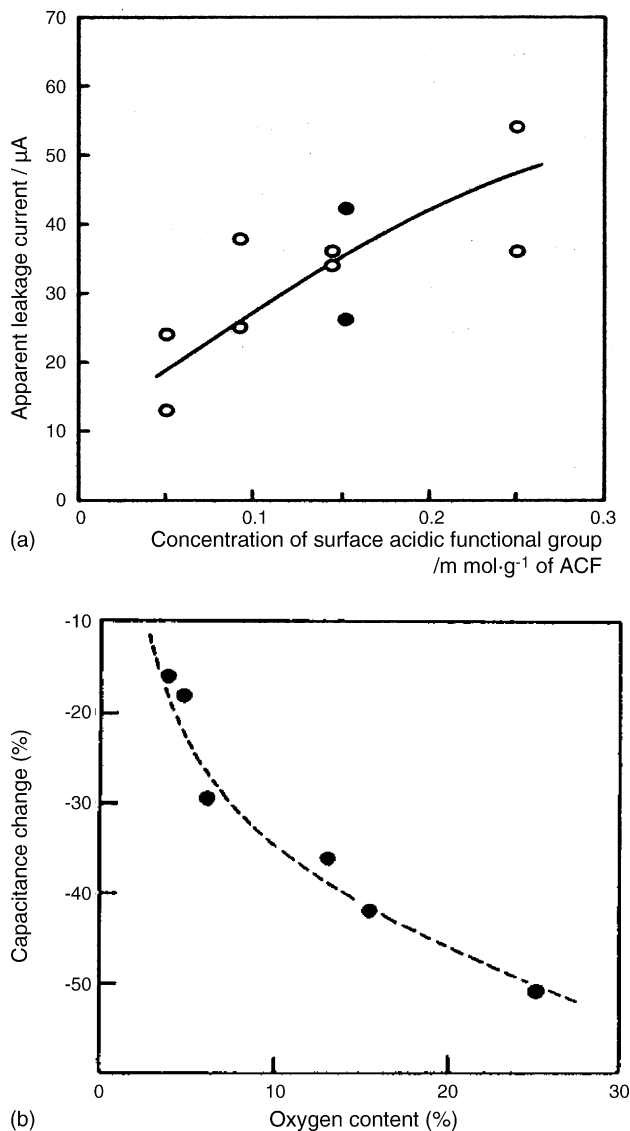


Fig. 4. Top: relationship between concentration of acidic functional groups on ACF electrode and leakage current of corresponding double-layer capacitor [62]. Bottom: influence of the oxygen content of activated carbons used for electrode on capacitance after application of 2.8 V at 70 °C for 1000 h [63].

strongly the rate and mechanism of capacitor self-discharge (or leakage) [5]. In particular, carbons with a high concentration of acidic surface functionalities are prone to exhibit high rates of self-discharge (Fig. 4(a)). The increase in leakage current suggests that the oxygen functional groups may serve as active sites, which can catalyze the electrochemical oxidation or reduction of the carbon, or the decomposition of the electrolyte components [62–64]. Conversely, the removal of oxygenated surface functionalities by high-temperature treatment in an inert environment results in lower leakage currents [62,65]. The presence of oxygenated functional groups can also contribute to capacitor instability, which results in an increased ESR and deterioration of capacitance [63–65]. The removal of oxygen from the carbons used in supercapacitor electrodes generally improves their stability (Fig. 4(b)).



Oxygen surface functional groups have also been shown to influence the rest potential of activated carbons [66]. The rest potential of activated carbons was found to be proportional to the logarithm of the oxygen content or to the concentration of acidic surface sites. Carbons with a high rest potential will experience undesirably higher voltages when charged and this could lead to gas generation.

Whilst charge storage on carbon electrodes is predominantly capacitive, there are also contributions from surface functional groups that can be rapidly charged and discharged and give rise to pseudocapacitance [13,67]. Various oxidative treatments have been applied to carbons [58,68–70], but it is often difficult to isolate the chemical changes from the physical and structural changes that frequently accompany oxidative treatments. Hsieh and Teng [64] used a relatively mild oxidative technique to oxidize polyacrylonitrile-activated carbon fabrics without introducing significant physical changes to the carbon. It was found that the Faradaic current, a direct measure of pseudocapacitance, increased significantly with the extent of oxygen treatment, while the change in double-layer capacitance was only minor. The large increase in specific capacitance (from  $\sim 120$  to  $150 \text{ F g}^{-1}$ ) was, however, accompanied by undesirable increases in internal resistance and leakage current.

#### 4.1.5. Double-layer capacitance of carbon materials

It is usually anticipated that the capacitance of a porous carbon (expressed in  $\text{F g}^{-1}$ ) will be proportional to its available surface-area (in  $\text{m}^2 \text{ g}^{-1}$ ). Whilst this relationship is sometimes observed [44,71], in practice it usually represents an oversimplification [30,72,73]. The major factors that contribute to what is often a complex (non-linear) relationship are: (i) assumptions in the measurement of electrode surface-area; (ii) variations in the specific capacitance of carbons with differing morphology; (iii) variations in surface chemistry (e.g., wettability and pseudocapacitive contributions discussed above); (iv) variations in the conditions under which carbon capacitance is measured.

The surface areas of porous carbons and electrodes are most commonly measured by gas adsorption (usually nitrogen at 77 K) and use BET theory to convert adsorption data into an esti-

mate of apparent surface-area. Despite its widespread use, the application of this approach to highly porous (particularly microporous) and heterogeneous materials has some limitations [74], and is perhaps more appropriately used as a semi-quantitative tool. Possibly the greatest constraint in attempting to correlate capacitance with BET surface-area, is the assumption that the surface-area accessed by nitrogen gas is similar to the surface accessed by the electrolyte during the measurement of capacitance. While gas adsorption can be expected to penetrate the majority of open pores down to a size that approaches the molecular size of the adsorbate, electrolyte accessibility will be more sensitive to variations in carbon structure and surface properties [75]. Electrolyte penetration into fine pores, particularly by larger organic electrolytes, is expected to be more restricted (due to ion sieving effects) and vary considerably with the electrolyte used [76]. Variations in electrolyte–electrode surface interactions that arise from differing electrolyte properties (viscosity, dielectric constant, dipole moment) will also influence wettability and, hence, electrolyte penetration into pores.

The specific double-layer capacitance (expressed per unit of BET area, in  $\mu\text{F cm}^{-2}$ ) of a range of carbon materials is listed in Table 5. The reported values vary considerably and appear to be highly dependent on carbon morphology. Most notably, the double-layer capacitance of the edge orientation of graphite is reported to be an order of magnitude higher than that of the basal layer [61,77]. One determinant of specific double-layer capacitance could therefore be the relative density of edge and basal plane graphitic structures in carbon materials. Carbons with a higher percentage of edge orientations (i.e., high  $L_c/L_a$  ratio) could be expected to exhibit a higher capacitance.

The low capacitance recorded when the basal layer of graphite is exposed to solution has been examined in detail by Randin and Yeager [78,79]. By treating basal plane carbon as a semi-conductor, they were able to show that there is a distribution of charge carrier concentration (charge density) that gives rise to a semi-conducting space-charge region on the carbon side of the interface. This means that some of the applied potential extends into the carbon and a space-charge capacitance ( $C_{sc}$ ) develops. This capacitance is in series with other capac-

Table 5  
Typical values for electrochemical double-layer capacitance of carbonaceous materials [5]

Carbonaceous material	Electrolyte	Double-layer capacitance ( $\mu\text{F cm}^{-2}$ ) <sup>a</sup>	Remarks
Activated carbon	10% NaCl	19	Surface-area $1200 \text{ m}^2 \text{ g}^{-1}$
Carbon black	1 M $\text{H}_2\text{SO}_4$	8	Surface-area $80\text{--}230 \text{ m}^2 \text{ g}^{-1}$
	31 wt.% KOH	10	
Carbon fiber cloth	0.51 M $\text{Et}_4\text{NBF}_4$ in propylene carbonate	6.9	Surface-area $1630 \text{ m}^2 \text{ g}^{-1}$
Graphite			
Basal plane	0.9 N NaF	3	Highly oriented pyrolytic graphite
Edge plane	0.9 N NaF	50–70	
Graphite powder	10% NaCl	35	Surface-area $4 \text{ m}^2 \text{ g}^{-1}$
Graphite cloth	0.168 N NaCl	10.7	Surface-area $630 \text{ m}^2 \text{ g}^{-1}$
Glassy carbon	0.9 N NaF	$\sim 13$	Solid
Carbon aerogel	4 M KOH	23	Surface-area $650 \text{ m}^2 \text{ g}^{-1}$

<sup>a</sup> Values based on estimates. For a comprehensive discussion see Ref. [48].

itive components of the double-layer, namely, the Helmholtz ( $C_H$ ) and diffuse ( $C_{diff}$ ) double-layer contributions. In effect, the stored charge, at a given potential, is spread over an additional dielectric element. The capacitance of the electrode ( $C$ ) is then represented as

$$\frac{1}{C} = \frac{1}{C_{sc}} + \frac{1}{C_H} + \frac{1}{C_{diff}} \quad (5)$$

For the semi-conducting basal graphite layer, the space-charge capacitance is significantly less than  $C_{diff}$  and  $C_H$ , and therefore dominates the overall interface capacitance. In fact, Randin and Yeager's calculations show that at the point of zero charge essentially all of the potential is associated with the space-charge region within the carbon electrode. By contrast, the edge orientation of graphite has a higher charge carrier density since its conductivity is more like that of a metal. The space-charge capacitance is correspondingly greater so that the overall interface capacitance is now dominated by  $C_{diff}$  and  $C_H$ .

The original work by Randin and Yeager was later re-examined by Gerischer [80], this time treating carbon as a metal and applying density-of-states arguments. While this treatment produced similar capacitance results to the earlier work, it also allowed Kötz and Hahn [81,82] to explain some of the behaviour of carbon in greater detail. In particular, these authors noted that the magnitude of both the capacitance and the conductivity can be directly related to the density of electronic states. Further, this treatment also provides an explanation for the observation that capacitance and conductivity both vary strongly with potential and exhibit minima close to the potential of zero charge (pzc). Central to this behaviour is the conclusion that both properties are essentially limited by the number of available charge carriers within the carbon space-charge region. This limitation is alleviated at potentials either side of the pzc because charging of the carbon electrode increases the numbers of available charge carriers. The authors also indicate that these relationships have important ramifications for the future development of carbon-based supercapacitor electrodes. For example, as carbons are activated to greater degrees, the pore walls become thinner. As a result, the effective thickness of the electrode material becomes similar to the dimensions of the space-charge region (defined by the Fermi length, and approximately equivalent to one graphene layer). In this situation, space-charge regions begin to overlap and less capacitance is generated per unit electrode area. This explanation is consistent with the smaller than expected capacitance often observed for highly activated carbon materials with extremely large surface areas (and correspondingly thinner pore walls) [81,83].

The measurement of carbon capacitance is also very dependent on the experimental conditions employed. For example, Fig. 5 demonstrates that the capacitance values measured for a range of porous carbons can vary substantially with discharge current [84]. The capacitance of microporous carbons are particularly affected by variations in discharge current due to the greater possibility of restricted electrolyte diffusion in narrower pores. Ideally, reported capacitance values of carbon

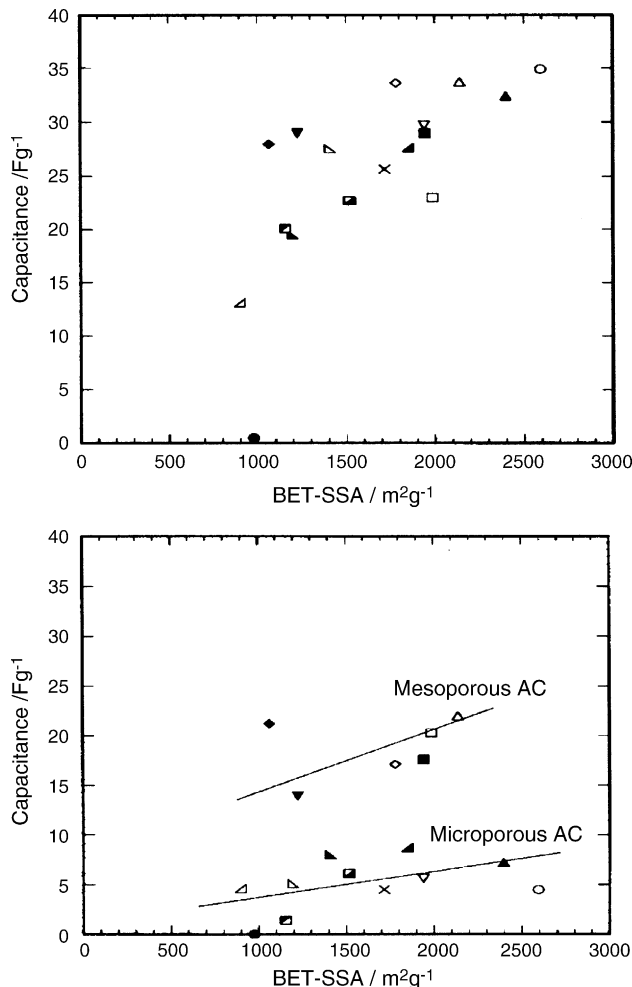


Fig. 5. Relationship between capacitance and BET surface-area of activated carbons measured at different current densities [135]. Top: low discharge current (10 mA); bottom: high discharge current (160 mA).

electrodes, particularly when used for comparative purposes, should be measured and compared at a fixed current density.

#### 4.2. Carbon surface-area and porosity

Porous carbons (particularly activated forms) are characterized by extremely large BET surface areas, that range from 500 to  $\sim 3000 \text{ m}^2 \text{ g}^{-1}$ . This surface-area largely arises from a complex interconnected network of internal pores. The IUPAC [85] classifies pores into three classes: micropores (diameters less than 2 nm), mesopores (diameters between 2 and 50 nm) and macropores (diameters greater than 50 nm).

Micropores have a high surface-area to volume ratio and, consequently, when present in significant proportions are a major contributor to the measured area of high surface-area activated carbons. Micropore sizes extend down to molecular dimensions and play an important role in the selectivity of adsorption-based processes, through restricted diffusion and molecular sieve effects. Fine micropores also exhibit a greater adsorbent–adsorbate affinity due to the overlap of adsorption

forces from opposing pore walls [86]. Accordingly, adsorption in fine pores can occur via a pore filling mechanism rather than solely by surface coverage (as is assumed by the Langmuir and BET calculations of surface-area). In such cases, the conversion of adsorption data into an estimate of surface-area, by the application of the BET equation, can lead to unrealistically high surface-area estimates.

Mesopores also contribute to surface-area and their relatively larger size also allows improved adsorbate accessibility by providing wider transport pores for diffusion. Macropores generally make a negligible contribution to the surface-area of porous carbons and their main function is to act as transport avenues into the interior of carbon particles.

While activated carbons, particularly those derived from naturally occurring precursors, tend to contain pores from all three size classes, careful selection of the carbon precursor and the activation conditions does allow significant control over the relative contribution of each size class. Materials with the highest surface-area are consistently obtained from highly microporous activated carbons, with high pore volumes, in which >90% of the total pore volume arises from microporosity.

As discussed earlier, while the vast majority of open pores can contribute to the measured surface-area, not all pores are electrochemically accessible. Ultimately, pore sizes will approach the double-layer dimensions, with the result that the movement of electrolyte will be restricted and, eventually, there will be a limitation on the ability of the electrolyte to form a double-layer. The surface-area arising from pores in this size range (which are dependent on electrolyte molecular dimensions) would not be effectively utilized and is unlikely to contribute to double-layer capacitance.

Studies on micropore accessibility in aqueous solvents have concluded that, generally, pores >0.5 nm are available for the electro-adsorption of simple hydrated ions [76,87]. A further study also concluded that the optimal pore-size range for double-layer capacitance of a carbon aerogel in aqueous H<sub>2</sub>SO<sub>4</sub> was between 0.8 and 2.0 nm [88]. The electrode material capacitance observed with organic electrolytes is generally less than the corresponding value in an aqueous electrolyte [7]. This difference is generally attributed to the larger overall diameter of the solvated organic electrolyte ions, which results in limited access to smaller pores. Whilst there is considerable debate over the lower size limit of pores that can be accessed by organic electrolytes, it is apparent from the high capacitances regularly reported for highly microporous carbons [30,44] that a significant portion of carbon microporosity (i.e., pores <2 nm) must also be accessible to organic electrolytes. Salitra et al. [76] have proposed that a de-solvation of organic electrolytes may occur to reduce ion dimensions and facilitate ‘forced electro-adsorption’ into smaller pores.

Narrow micropores will only be accessed through an appreciable ‘solution resistance’ arising from hindered or restricted electrolyte diffusion within these narrow pores. This will contribute directly to a high time constant (poor frequency response), and hence a low rate capability due to the retardation of the movement of ions in the pores during charging/discharging. Therefore, these pores will only make a minor

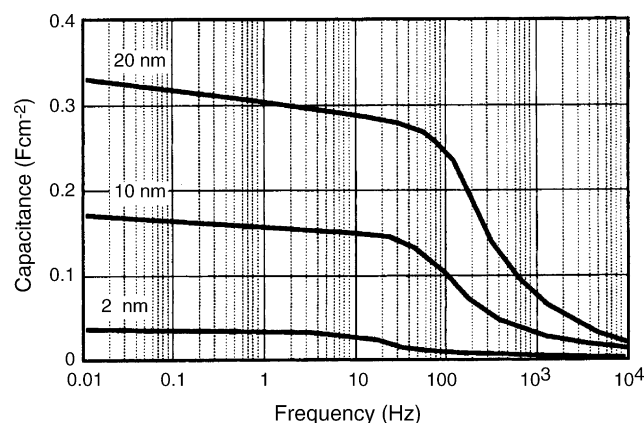


Fig. 6. Effect of pore diameter on the capacitance vs. frequency performance of single porous electrode [13].

contribution to charge-storage capacity under high-rate, or short duration, power pulse discharge or recharge [5].

In electrochemical capacitors based on porous electrodes, an unavoidable distributed electrolyte resistance arises that extends into the depth of the pore. This resistance ( $R$ ) is coupled with distributed interfacial capacitance ( $C$ ) elements and leads to an electrode with a non-uniform distribution of effective resistance and capacitance (commonly referred to as the ‘transmission line model’). A distributed RC network then arises that restricts the rate of charge and discharge. This situation has also been described as a ‘penetration effect’ and limits the power capability of the system [89–92]. At low charge rates, or frequencies, electrolyte ions have time to penetrate into the depth of the pores and additional surface-area is accessed (and distributed resistance is also at a maximum). As the charge rate or frequency increases, electrolyte penetration becomes poorer and less surface-area is accessed. Similarly, larger pores lead to a lower distributed electrolyte resistance and greater electrolyte penetration that enables the majority of the surface-area, and hence the capacitance, to be utilized (Fig. 6) [13,93].

Clearly, the pore-size distribution of porous carbons influences to a large degree the fundamental performance criteria of carbon-based supercapacitors, i.e., the relationship between power and energy density, and the dependence of performance on frequency. Not surprisingly, therefore, considerable research is presently being directed towards the development of carbon materials with a tailored pore-size distribution to yield high capacitance and low resistance electrodes.

#### 4.3. Carbon forms

To a large extent, carbons used in commercial supercapacitors have remained proprietary, but most would appear to be a form of activated carbon which is often blended with a conductive carbon black or graphite. Activated carbons obtained from carbonized phenolic resins or petroleum cokes appear to be particularly suitable, especially for organic-based systems [15,63]. Other forms, or blends of carbons, are also employed and the properties of selected carbons are discussed in greater detail below.

#### 4.3.1. Carbon blacks

Carbon blacks are a group of materials that are characterized by having near spherical carbon particles of colloidal size, which are produced by the partial combustion or thermal decomposition of hydrocarbons (usually gases, oils, or distillates) in the gas phase [94,95]. During production, the colloidal carbon particles coalesce into chemically fused aggregates and agglomerates (groups of aggregates) with varying morphologies. Their fundamental properties vary with feedstock and manufacturing conditions, and they are usually classified according to their method of preparation or intended application. The key properties of carbon blacks are considered to be fineness (primary particle size), structure (aggregate size/shape), porosity, and surface chemistry.

Carbon blacks are routinely used as conductive fillers in many types of battery and supercapacitor electrodes [6,16,96,97]. Highly conductive carbon blacks are characterized by a high structure (i.e., aggregates with a highly branched, open structure), high porosity, small particle size, and a chemically clean (oxygen free) surface. The conductivity of carbon blacks is typically in the range  $10^{-1}$  to  $10^2$  ( $\Omega \text{ cm}$ )<sup>-1</sup> [95] and is influenced by the relative ability of electrons to jump the gap between closely-spaced aggregates (electron tunnelling) and by graphitic conduction via touching aggregates. The loading of carbon black is of critical importance because, at low loadings, the average inter-aggregate gap is too large for the carbon black to influence the conductivity of the composite. As the loading is increased, a percolation threshold (i.e., critical loading) is reached whereby the conductivity increases rapidly up to a limiting value. High porosity and/or finer carbon blacks have more particles per unit weight and, therefore, reduce the average gap width between aggregates due to their greater number [94,95].

The surface-area (BET) of carbon blacks covers a wide range i.e., from <10 to greater than  $1500 \text{ m}^2 \text{ g}^{-1}$  [48,98]. The porosity in carbon blacks also varies from mild surface pitting to the actual hollowing out of particles. Additional porosity is also created by the intra- and inter-aggregate voids that are formed between the small, fused, primary carbon particles. The surface-area of carbon blacks is generally considered to be more accessible than other forms of high surface-area carbon [98]. Supercapacitor electrodes have been produced from high surface-area blacks (containing a binder) with specific capacitances of up to  $250 \text{ F g}^{-1}$ ; corresponding to double-layer capacitances in the range of  $10\text{--}16 \mu\text{F cm}^{-2}$  [98,99]. On the other hand, the low compacted density of high surface-area blacks and the high level of binder often required to produce mechanically stable electrodes, typically results in electrodes with low electrical conductivities and volumetric capacitance.

The fine, highly branched structure of carbon blacks make them ideally suited to filling inter-particle voids created between coarse particles. As well as improving the electrical contact between particles, the addition of carbon blacks also allows some manipulation of the inter-particle void volume that exists in carbon electrodes that can account for  $\sim 25\text{--}40\%$  of the total electrode volume. Whilst some voidage is essential in carbon electrodes, to act as an 'electrolyte reservoir' and provide access to the internal porosity of carbon particles, an excessive amount

can reduce both the volumetric and gravimetric energy density of the device. Partially filling these voids with a porous carbon black will not only provide additional capacitance, but will also displace excess electrolyte that would otherwise completely fill the voids and increase the wet electrode weight and ultimately the cell cost.

#### 4.3.2. Carbon aerogels

Carbon aerogels are highly porous materials prepared by the pyrolysis of organic aerogels. They are usually synthesized by the poly-condensation of resorcinol and formaldehyde, via a sol-gel process, and subsequent pyrolysis [100,101]. By varying the conditions of the sol-gel process, the macroscopic properties of aerogels (density, pore size and form (shape/size)) can be controlled. The aerogel solid matrix is composed of interconnected colloidal like carbon particles or polymeric chains. After pyrolysis, the resulting carbon aerogels are more electrically conductive than most activated carbons [47,102]. Carbon aerogels derived from the pyrolysis of resorcinol-formaldehyde are preferred as they tend to have the highest porosity, high surface-area ( $400\text{--}1000 \text{ m}^2 \text{ g}^{-1}$ ), uniform pore sizes (largely between 2 and 50 nm) and high density. They can also be produced as monoliths, composites, thin films, powders or micro-spheres.

The versatility of the sol-gel process, and the diversity of forms, enables the construction of carbon electrodes from aerogel powders using a binder, or the manufacture of monolithic, binder-less electrodes. Thin and mechanically stable aerogel electrodes, with a thickness in the range of several hundred microns, can also be prepared by the integration of carbon fibres or woven fabrics in the sol-gel precursor [103–105].

Electrochemical studies on carbon aerogels have reported [106,107] that capacitance is more strongly correlated with mesopore surface-area than with the total BET surface-area. These studies showed that carbon aerogels with pore diameters in the range  $\sim 3\text{--}13 \text{ nm}$  exhibited stable capacitive behaviour and the highest capacitances.

Several investigations have increased the surface-area of carbon aerogels by thermal activation [101,108]. Nevertheless, while the activation of carbon aerogels resulted in a large increase in BET surface-area, from  $\sim 650$  to  $\sim 2500 \text{ m}^2 \text{ g}^{-1}$ , the accompanying increase in specific capacitance was relatively small. The corresponding double-layer charge storage capacity also decreased from  $18 \mu\text{F cm}^{-2}$  for the unactivated sample to  $8 \mu\text{F cm}^{-2}$  after activation, and this was attributed to an increase in inaccessible pores in the latter sample. Further examination of the activated sample revealed considerable changes in surface morphology and a large increase in microporosity. It was also found that whilst a greater degree of activation increases the surface-area ( $\text{m}^2 \text{ g}^{-1}$ ) of the carbon aerogels, the resulting volumetric capacitance actually passes through a maximum (in this case  $\sim 50 \text{ F cm}^{-3}$ ) at surface areas of around  $1000 \text{ m}^2 \text{ g}^{-1}$ .

#### 4.3.3. Carbon fibres

As opposed to vapour-grown fibres, commercial carbon fibres are usually produced from thermosetting organic materials such as cellulose (or rayon), phenolic resins, polyacrylonitrile (PAN)- and pitch-based materials [109]. The preparation of carbon

fibres basically consists of preparing a precursor solution or melt, the extrusion of this material through a die or spinnerette, and the drawing of extrudant into a thin fibre. After stabilization (200–400 °C) and carbonization (800–1500 °C), the raw fibre can be activated in a controlled oxidizing environment at 400–900 °C, or can be graphitized (at elevated temperatures up to 3000 °C).

The quality of the carbon fibre depends on the structure and assembly of aromatic constituents and their alignment, and these factors, in turn, are influenced by the precursor and the manufacturing process. In general, carbon fibres derived from pitch typically provide better electrical properties than those obtained from hard carbons such as PAN [48,109]. In addition, fibres derived from phenolic resins have a lower concentration of acidic surface functional groups and a high surface-area [62,110].

Activated carbon fibres (ACF) have a typical diameter of  $\sim 10 \mu\text{m}$  and a very narrow pore-size distribution that is predominantly microporous ( $< 2 \text{ nm}$ ). Due to the limited fibre dimensions, the porosity of ACFs is largely situated at the surface of the fibre and thereby provides good accessibility to active sites. Unlike particulate forms of activated carbon, both the pore diameter and pore length can be more readily controlled in ACFs. These features make ACFs very attractive electrode materials as both high adsorption capacities and adsorption rates are obtainable [15]. By contrast, the outer surface of particulate carbons is more extensively oxidized during activation. This creates larger macropores and places the fine porosity towards the centre of the particle.

Carbon fibres are available in many forms, e.g., tow (bundles), chopped fibre, mat, felt, cloth, and thread. ACF cloths (bundles of fibres woven into a textile form and activated) with surface areas up to  $2500 \text{ m}^2 \text{ g}^{-1}$  are now commercially available [15]. Compared with electrodes prepared from powdered carbons ACFs offer the advantages of high surface-area, good electrical conductivity, and ease of electrode formation and containment. On the other hand, the cost of ACF products is generally higher than that of powdered forms of carbon.

Although AC fibres and cloths have a low electrical resistance along the fibre axis, the contact resistance between the fibres can be an issue unless the fibres are kept in close contact, usually by some sort of containment pressure. Similarly, good electrical contact is required between the carbon cloth and the metal collector. ACF cloths are sometimes coated on one side with a thin layer of metal (e.g., by plasma spraying) to improve electrical contact with the collector [110].

#### 4.3.4. Glassy carbons

Glassy carbon (also referred to as vitreous or polymeric carbon) is produced by the thermal degradation of selected polymers resins; typically, phenolic resins or furfuryl alcohol are used. The precursor resin is cured, carbonized very slowly, and then heated to elevated temperatures. The physical properties of glassy carbons are generally dependent on the maximum heat treatment temperature, which can vary from 600 to 3000 °C. It appears that temperatures around 1800 °C produce glassy carbons with more desirable properties [48,111–113].

Glassy carbons have little accessible surface-area and a relatively low density ( $\sim 1.5 \text{ g cm}^{-3}$  cf., graphite  $2.26 \text{ g cm}^{-3}$ ); which is attributed to the presence of a significant volume of isolated ‘closed’ pores ( $\sim 30\%$  v/v). These pores are typically 1–5 nm in size and are formed by the cavities created by randomly oriented and inter-twined graphene sheets. The resulting structure is very rigid and provides glassy carbons with tensile and compressive strengths that are typically higher than those for graphite. Glassy carbon also has a very low electrical resistivity ( $(\sim 3\text{--}8) \times 10^{-4} \Omega \text{ cm}$  [48]) and is therefore particularly suited for high-power supercapacitors that require a low internal resistance [114]. Another attractive feature of glassy carbon is that it can be produced as free-standing films or thin sheets as well as powders [111,115].

The isolated porosity of glassy carbons can be opened by thermal or electrochemical oxidation processes (activation) to give a material with a high specific surface-area that is well suited as an EDLC electrode material [116,117]. Thermal activation appears to provide a wider, more accessible porosity than electrochemical oxidation processes. Consequently, electrodes that utilize electrochemically activated samples generally exhibit greater ionic resistance, particularly at high frequencies and when non-aqueous electrolytes are used [114]. Volumetric surface areas of  $\sim 1800 \text{ m}^2 \text{ cm}^{-3}$  and double-layer capacitances of  $\sim 20 \mu\text{F cm}^{-2}$  have been achieved for thermally oxidized glassy carbons [111,116].

During the activation of glassy carbon, a film with open pores is created on the surface. The growth and thickness of this active film can be controlled by the diffusion of the oxidant into the film. If a glassy carbon sheet is activated, the film that develops at the surface remains well connected (both mechanically and electrically) to the underlying carbon substrate, which now acts as an electrically conducting support for the active layer. The resulting monolithic, electrode and current-collector assembly is no longer limited by grain-to-grain contact resistance and is an attractive electrode option for high-power supercapacitors.

#### 4.4. Carbon nanostructures

Carbon nanotubes and nanofibres are produced by the catalytic decomposition of certain hydrocarbons. By careful manipulation of various parameters, it is possible to generate nanostructures in assorted conformations and also control their crystalline order [118].

There is considerable interest in the application of carbon nanotubes (CNTs) as electrode materials for supercapacitors and other energy-storage devices [119–123]. The nanoscale tubular morphology of these materials can offer a unique combination of low electrical resistivity and high porosity in a readily accessible structure. Single-walled (SWNT) and multi-walled nanotubes (MWNTs) have been studied as electrode materials in both aqueous and non-aqueous electrolytes.

The specific capacitance of CNTs has been shown to be highly dependent on their morphology and purity [124]. For purified nanotubes (i.e., without residual catalyst or amorphous carbon), the specific capacitance varies typically from 15 to  $80 \text{ F g}^{-1}$  with surface areas that range from  $\sim 120$  to  $400 \text{ m}^2 \text{ g}^{-1}$  [124,125]. The

surface-area of CNTs is predominantly “mesoporous” and is associated with the exterior of the tubes; the voids arise from the entangled nanotubes and, in some cases, from the presence of an accessible central canal. Specific capacitance can be increased to  $\sim 130 \text{ F g}^{-1}$  by subsequent oxidative treatment (e.g., with nitric acid) which modifies the surface texture of the CNTs and introduces additional surface functionality, which is capable of contributing to pseudocapacitance [125–127].

Niu et al. [128] produced catalytically-grown MWNTs with a diameter of 8 nm and a BET surface-area of  $\sim 250 \text{ m}^2 \text{ g}^{-1}$ . The tubes were subsequently treated with nitric acid and formed into electrodes that consisted of freestanding mats of entangled nanotubes with an increased surface-area of  $430 \text{ m}^2 \text{ g}^{-1}$ . The electrode mat contained negligible microporosity and had an average pore diameter of 9.2 nm, which is 1.2 nm larger than the diameter of the nanotube itself. Therefore, unlike other types of carbon electrodes that may contain micropores, slit-shaped pores or dead-end pores which are difficult to access, much of the porosity in the nanotube mats is due to the interstitial spaces created by the entangled nanotube network. This open porosity is readily accessible to electrolytes. The specific capacitance of the nanotube mat electrodes in sulfuric acid was determined to be  $102 \text{ F g}^{-1}$  (at 1 Hz) and this corresponds to a double-layer capacity of  $24.2 \mu\text{F cm}^{-2}$ . The same cell also had an estimated power density of  $>8 \text{ kW kg}^{-1}$ .

In order to improve their capacitance, carbon nanotubes have been chemically activated with potassium hydroxide. The treatment can substantially increase the surface-area of carbon nanotubes (by a factor of  $\sim$ two to three times) whilst maintaining a nanotubular morphology [125,129]. Whereas the treatment appears to have little effect on nanotube diameter, it can considerably shorten the length and is accompanied by the development of cracks and surface irregularities through a partial erosion of the outer carbon layers [129]. Frackowiak et al. [125] managed to increase the BET surface-area of MWNTs from an initial value of 430 to  $1035 \text{ m}^2 \text{ g}^{-1}$  by activation with potassium hydroxide. Whilst the product still maintained a high degree of mesoporosity, the activation process also introduced considerable microporosity. The specific capacitance of the material was  $90 \text{ F g}^{-1}$  ( $8.7 \mu\text{F cm}^{-2}$ ) in alkaline media but was limited to  $65 \text{ F g}^{-1}$  ( $6.2 \mu\text{F cm}^{-2}$ ) in non-aqueous media.

SWNTs have been prepared as composites with polyvinylidene chloride (PVDC). After carbonisation, the composite electrodes exhibited a maximum specific capacitance of  $180 \text{ F g}^{-1}$  and a measured power density of  $20 \text{ kW kg}^{-1}$  in potassium hydroxide [121,122,130]. The high specific capacitance, for an electrode material with a surface-area of only  $357 \text{ m}^2 \text{ g}^{-1}$ , was attributed to an increased surface-area and a redistribution of CNT pore size to smaller, more optimal, values near 3–5 nm [121].

Limitations in the effective surface-area of CNTs has prompted studies into the preparation of nanocomposites of CNTs with conducting polymers [121,131]. These composites realize a large capacitance, by combining the electric double-layer capacitance of the CNTs and the redox capacitance of the conducting polymer [120]. They are typically prepared by the in situ chemical polymerization of a suitable monomer

which generally forms a uniform coating onto the nanotube surface. MWNTs, electrodeposited with a thin porous layer of polypyrrole (Ppy), have been prepared with a specific capacitance of  $\sim 170 \text{ F g}^{-1}$  [123,124]. This value is considerably greater than the corresponding values for pristine MWNTs or Ppy alone. Similarly, SWNT-Ppy nanocomposites have been produced with specific capacitances up to  $265 \text{ F g}^{-1}$  [120,121]. In these nanocomposites, the Ppy also acts as a conducting agent and contributes to the specific capacitance by reducing the internal resistance of the supercapacitor [121].

As with other forms of particulate carbon, carbon nanotubes are usually formed into electrodes using rather tedious binder-enriched, or binderless, fabrication methods. Both these methods of electrode fabrication result in a high contact resistance between the active material and the current collector. An attractive form of carbon nanotube electrode can be obtained by growing the nanotubes directly on to a conductive substrate. This approach minimizes the contact resistance between the active material and the current-collector and greatly simplifies electrode fabrication [132,133].

Carbon nanotubes, uniformly 50 nm in diameter, have been grown on graphite foil [132,134]. Subsequent testing of the resulting composite electrode confirmed a high specific capacitance of  $115.7 \text{ F g}^{-1}$  (1 M  $\text{H}_2\text{SO}_4$ ) and good electrochemical stability. Emmenegger et al. [133] have also successfully grown well-aligned carbon nanotube films on aluminium supports. These nanotubes were multi-walled with lengths in the range 1–10  $\mu\text{m}$  and diameters between 5 and 100 nm. A supercapacitor, constructed from the nanotube-coated aluminium electrode gave a volumetric capacitance of  $120 \text{ F cm}^{-3}$  and a very high power density.

Although there are good indications that EDLC devices constructed from carbon nanotubes may offer power capabilities well above  $8 \text{ kW kg}^{-1}$  [122,128], their specific energies are highly dependent on their method of preparation and are generally lower than the levels achieved from more conventional high surface-area carbons. This, in addition to their limited availability and high cost, presently limits their commercial utilization.

## 5. Summary

Carbon, in its various forms, is the most extensively examined and widely utilised electrode material in supercapacitors. Continuing efforts are aimed at achieving higher surface-area with lower matrix resistivity at an acceptable cost. Carbons with BET surface areas of up to  $3000 \text{ m}^2 \text{ g}^{-1}$  are available in various forms, viz., powders, fibres, woven cloths, felts, aerogels, and nanotubes. Even though surface-area is a key determinant of capacitance, other factors such as carbon structure, pore size, particle size, electrical conductivity and surface functionalities also influence capacitance and ultimately supercapacitor performance. Carbon materials that have both a high surface-area and good electrolyte accessibility (favourable distribution of appropriately sized pores) allow the optimum amount of charge to be stored and delivered.

The majority of commercial carbons can be described as ‘engineered carbons’. These are manufactured and have an

amorphous structure with a more or less disordered microstructure, which is based on that of graphite and can be viewed as sections of hexagonal carbon layers with little long-range order parallel to the layers. The selection of the carbon precursor and the processing conditions will influence the size of the graphene sheets, their degree of stacking (into graphitic micro-crystallites) and the relative orientation of these crystallites. The size and orientation of the graphitic crystallites strongly influences carbon properties and defines the texture, porosity, surface-area, capacitance and electrical conductivity.

The presence of surface groups on carbons modifies the electrochemical interfacial state of the carbon surface and its double-layer properties, e.g., wettability, point of zero charge, adsorption of ions (capacitance) and self-discharge characteristics. Whilst the presence of oxygenated species on the surface of porous carbons is often linked to increases in capacitance (pseudocapacitance), this increase often leads to irreversible changes and, after prolonged cycling, can be accompanied by a progressive deterioration of capacitance and increases in equivalent series resistance and self-discharge rates.

Considerable research is presently being directed towards the development of carbon materials with a tailored pore-size distribution to yield electrodes with high capacitance and low resistance. The incorporation of redox materials (e.g., metal oxides or conducting polymers) into carbon electrodes is also receiving increased attention as a means of increasing capacitance, as is the tailoring of electrodes and electrolytes capable of operating at higher voltages (>3 V). Clearly, the goal is to enhance the specific energy of carbon-based supercapacitors without detracting from the present very high levels of specific power.

## Acknowledgements

The authors wish to acknowledge financial support from the CSIRO Energy Transformed National Research Flagship initiative.

## References

- [1] A.K. Shukla, Resonance 6 (2001) 72.
- [2] P.J. Mahon, C.J. Drummond, Aust. J. Chem. 54 (2001) 473.
- [3] A. Nishino, J. Power Sources 60 (1996) 137.
- [4] J. Nickerson, Proceedings of the Ninth International Seminar on Double Layer Capacitors and Similar Energy Storage Devices, Deerfield Beach, FL, 1999.
- [5] B.E. Conway, Electrochemical Supercapacitors—Scientific Fundamentals and Technological Applications, Kluwer, New York, 1999.
- [6] J.P. Zheng, Electrochem. Solid-State Lett. 2 (1999) 359.
- [7] M. Mastragostino, F. Soavi, C. Arbizzani, W. van Schalkwijk, B. Scrosati (Eds.), Advances in Lithium-ion Batteries, Kluwer Academic/Plenum Publishers, 2002, p. 481.
- [8] M. Mastragostino, C. Arbizzani, F. Soavi, Solid State Ionics 148 (2002) 493.
- [9] K. Naoi, Y. Oura, H. Tsujimoto, Proceedings of the Electrochemical Society, vol. 96-25, The Electrochemical Society, Pennington, NJ, 1996, p. 120.
- [10] X. Andrieu, Energy Storage Syst. Electron.: New Trends Electrochem. Technol. 1 (2000) 521.
- [11] S. Sarangapani, B.V. Tilak, C.-P. Chen, J. Electrochem. Soc. 143 (1996) 3791.
- [12] A. Burke, J. Power Sources 91 (2000) 37.
- [13] R. Kötz, M. Carlen, Electrochim. Acta 45 (2000) 2483.
- [14] M. Reimerink, Advanced Capacitor World Summit: Building the Technology Applications and New Business Opportunities for High Performance Electrochemical Capacitors (ECs), Washington, DC, 2003.
- [15] K. Otsuka, C.L. Segal, Advanced Capacitor World Summit: Building the Technology Applications and New Business Opportunities for High Performance Electrochemical Capacitors (ECs), Washington, DC, 2003.
- [16] A.S. Fialkov, Russ. J. Electrochem. 36 (2000) 389.
- [17] H. von Helmholtz, Ann. Phys. (Leipzig) 89 (1853) 211.
- [18] G. Gouy, J. Phys. 9 (1910) 457.
- [19] D.L. Chapman, Phil. Mag. 25 (1913) 475.
- [20] O. Stern, Zeit. Elektrochem. 30 (1924) 508.
- [21] D.C. Grahame, Chem. Rev. 41 (1947) 441.
- [22] J.O. Bockris, M.A. Devanathan, K. Muller, Proc. R. Soc. A274 (1963) 55.
- [23] H.I. Becker, Low voltage electrolytic capacitor, United States Patent 2,800,616 (1957).
- [24] R.A. Rightmire, Electrical energy storage apparatus, United States Patent 3,288,641 (1966).
- [25] D.L. Boos, S.D. Argade, International Seminar on Double Layer Supercapacitors and Similar Energy Storage Devices, Florida Educational Seminars, Deerfield Beach, FL, 1991, p. 1.
- [26] D.L. Boos, Electrolytic capacitor having carbon paste electrodes, United States Patent 3,536,963 (1970).
- [27] M. Endo, T. Takeda, Y.J. Kim, K. Koshiba, K. Ishii, Carbon Sci. 1 (2001) 117.
- [28] M.F. Rose, Proceedings of the 33rd International Power Sources Symposium, Pennington, NJ, 1988, p. 572.
- [29] A.M. Namisnyk, B.E. Thesis, University of Technology, Sydney, Australia, 2003.
- [30] D. Qu, H. Shi, J. Power Sources 74 (1998) 99.
- [31] A.K. Shukla, S. Sampath, K. Vijayamohan, Curr. Sci. 79 (2000) 1656.
- [32] A. Burke, M. Arulepp, Proceedings of the Symposium on Batteries and Supercapacitors, San Francisco, CA, 2001, p. 576 (Notes: Paper Presented at the Electrochemical Society Meeting in San Francisco, September 2–5, 2001).
- [33] O. Haas, E.J. Cairns, Annu. Rep. Prog. Chem., Sect. C 95 (1999) 163.
- [34] B.E. Conway, J. Solid State Electrochem. 7 (2003) 637.
- [35] M.F. Rose, C. Johnson, T. Owens, B. Stephens, J. Power Sources 47 (1994) 303.
- [36] A.F. Burke, T.C. Murphy, Materials for Electrochemical Energy Storage and Conversion—Batteries, Capacitors and Fuel Cells: Symposium Held, April 17–20, 1995, San Francisco, CA, Materials Research Society, Pittsburgh, PA, 1995, p. 375.
- [37] B. McEnaney, T.D. Burchell (Eds.), Carbon Materials for Advanced Technologies, Pergamon, 1999, p. 1.
- [38] H.O. Pierson, Handbook of Carbon, Graphite, Diamond and Fullerenes, Noyes Publications, NJ, USA, 1993.
- [39] E. Fitzer, K.-H. Köchling, H.P. Boehm, H. Marsh, Pure Appl. Chem. 67 (1995) 473.
- [40] M. Inagaki, L.R. Radovic, Carbon 40 (2002) 2263.
- [41] H. Marsh, Introduction to Carbon Science, Butterworths, 1989.
- [42] X. Bourrat, H. Marsh, F. Rodriguez-Reinoso (Eds.), Science of Carbon Materials, Universidad de Alicante, 2000, p. 1.
- [43] R.C. Bansal, J.B. Donnet, F. Stoeckli, Active Carbon, Marcel Dekker, New York, 1988 (Chapter 2).
- [44] D. Lozano-Castelló, D. Cazorla-Amorós, A. Linares-Solano, S. Shiraishi, H. Kurihara, A. Oya, Carbon 41 (2003) 1765.
- [45] C.A. Leon y Leon, L.R. Radovic, Chemistry and Physics of Carbon, vol. 24, Marcel Dekker, New York, 1994, p. 213.
- [46] S. Biniak, A. Swiatkowski, M. Pakula, L.R. Radovic (Eds.), Chemistry and Physics of Carbon, vol. 27, Marcel Dekker, New York, 2001, p. 125.

- [47] T.D. Tran, K. Kinoshita, Proceedings of the Electrochemical Society, vol. 98-15, The Electrochemical Society, Pennington, NJ, 1998, p. 548.
- [48] K. Kinoshita, Carbon: Electrochemical and Physicochemical Properties, Wiley-Interscience, New York, 1988.
- [49] I.L. Spain, P.L. Walker, P.A. Thrower (Eds.), Chemistry and Physics of Carbon, vol. 16, Marcel Dekker, New York, 1981, p. 119.
- [50] A. Espinola, P.M. Miguel, M.R. Salles, A.R. Pinto, Carbon 24 (1986) 33.
- [51] W.M. Hess, C.R. Herd, J.B. Donet, R.C. Bansal, M.J. Wang (Eds.), Carbon Black, 2nd ed., Marcel Dekker, New York, 1993, p. 89.
- [52] K.H. Radeke, K.O. Backhaus, A. Swaitkowski, Carbon 29 (1991) 122.
- [53] M. Polovina, B. Babic, B. Kaluderovic, A. De Kanski, Carbon 35 (1997) 1047.
- [54] L. Bonnefoi, P. Simon, J.F. Fauvarque, C. Sarrazin, A. Dugast, J. Power Sources 79 (1999) 37.
- [55] X. Andrieu, L. Josset, Proc. Electrochem. Soc. 95-29 (1996) 181.
- [56] P.L. Taberna, P. Simon, J.F. Fauvarque, J. Electrochem. Soc. 150 (2003) A292–A300.
- [57] J.H. Kim, K.H. Shin, C.S. Jin, D.K. Kim, Y.G. Lim, J.H. Park, Y.S. Lee, J.S. Joo, K.H. Lee, Electrochemistry 69 (2001) 853.
- [58] K. Kinoshita, X. Chu, Proceedings of the Symposium on Electrochemical Capacitors, vol. 95-25, The Electrochemical Society, Pennington, NJ, 1995, p. 171.
- [59] P.E. Fanning, M.A. Vannice, Carbon 31 (1993) 721.
- [60] B.R. Puri, P.L. Walker (Eds.), Chemistry and Physics of Carbon, vol. 6, Marcel Dekker, New York, 1970, p. 191.
- [61] D. Qu, J. Power Sources 109 (2002) 403.
- [62] A. Yoshida, I. Tanahashi, A. Nishino, Carbon 28 (1990) 611.
- [63] T. Morimoto, K. Hiratsuka, Y. Sanada, K. Kurihara, J. Power Sources 60 (1996) 239.
- [64] C.-T. Hsieh, H. Teng, Carbon 40 (2002) 667.
- [65] T. Morimoto, K. Hiratsuka, Y. Sanada, K. Kurihara, T. Jimbo, Proceedings of the 183rd Meeting of the Electrochemical Society, vol. 93-23, Honolulu, Hawaii, 1993, p. 49.
- [66] M.W. Verbrugge, B.J. Koch, J. Electrochem. Soc. 146 (1999) 833.
- [67] B.E. Conway, Proceedings of the Symposium on Electrochemical Capacitors, vol. 95-29, The Electrochemical Society, Pennington, NJ, 1995, p. 15.
- [68] M. Ishikawa, A. Sakamoto, M. Morita, Y. Matsuda, K. Ishida, J. Power Sources 60 (1996) 233.
- [69] T. Momma, X. Liu, T. Osaka, Y. Ushio, Y. Sawada, J. Power Sources 60 (1996) 249.
- [70] K. Jurewicz, E. Frackowiak, Mol. Phys. Rep. 27 (2000) 36.
- [71] A. Yoshida, S. Nonaka, I. Aoki, A. Nishino, J. Power Sources 60 (1996) 213.
- [72] S. Shiraishi, H. Kurihara, A. Oya, Carbon Sci. 1 (2001) 133.
- [73] M. Endo, Y.J. Kim, T. Takeda, T.H.T. Maeda, K. Koshihara, H. Hara, M.S. Dresselhaus, J. Electrochem. Soc. 148 (2001) A1135–A1140.
- [74] S. Lowell, J.E. Shields, Powder Surface Area and Porosity, 3rd ed., Chapman & Hall, London, 1991.
- [75] J. Koresch, A. Soffer, J. Electrochem. Soc. 124 (1977) 1379.
- [76] G. Salitra, A. Soffer, L. Eliad, Y. Cohen, D. Aurbach, J. Electrochem. Soc. 147 (2000) 2486.
- [77] R.L. McCreery, K.K. Cline, P.T. Kissinger, W.R. Heineman (Eds.), Laboratory Techniques in Electroanalytical Chemistry, 2nd ed., Marcel Dekker, New York, 1995, p. 293.
- [78] J.-P. Randin, E. Yeager, Electroanal. Chem. Interfacial Electrochem. 36 (1972) 257.
- [79] J.-P. Randin, E. Yeager, Electroanal. Chem. Interfacial Electrochem. 58 (1975) 313.
- [80] H. Gerischer, J. Phys. Chem. 89 (1985) 4249.
- [81] R. Kötz, M. Hahn, O. Barbieri, J.-C. Sauter, R. Gallay, Proceedings of the 13th International Seminar on Double Layer Capacitors and Similar Energy Storage Devices, December 8–10, 2003, Deerfield Beach, FL, 2002.
- [82] M. Hahn, M. Baertschi, O. Barbieri, J.-C. Sauter, R. Kötz, R. Gallay, Electrochem. Solid State Lett. 7 (2004) A33–A36.
- [83] D. Qu, H. Shi, J. Power Sources 74 (1998) 99.
- [84] H. Tamai, Kouzu, M. Masayuki, H. Morita, Yasada, Electrochem. Solid State Lett. 6 (2003) A214–A217.
- [85] K.S.W. Sing, D.H. Everett, R.A.W. Haul, L. Moscou, R.A. Pierotti, J. Rouquerol, T. Siemieniewska, Pure Appl. Chem. 57 (1985) 603.
- [86] J.W. Patrick, Porosity in Carbons, Halsted Press, New York, 1995.
- [87] H. Shi, Electrochim. Acta 41 (1996) 1633.
- [88] C. Lin, J.A. Ritter, B.N. Popov, J. Electrochem. Soc. 146 (1999) 3639.
- [89] R. De Levies, Electrochim. Acta 8 (1963) 751.
- [90] R. De Levie, P. Delahay, C.W. Tobias (Eds.), Advances in Electrochemistry and Electrochemical Engineering, vol. 6, Interscience, New York, 1967, p. 329.
- [91] W.G. Pell, B.E. Conway, J. Power Sources 96 (2001) 57.
- [92] B.E. Conway, J. Electroanal. Chem. 524/525 (2002) 4.
- [93] S.-I. Pyun, C.-H. Kim, S.-W. Kim, J.-H. Kim, J. New Mater. Electrochem. Syst. 5 (2002) 289.
- [94] R. Taylor, H. Marsh, E.A. Heintz, F. Rodriguez-Reinoso (Eds.), Introduction to Carbon Technologies, Universidad de Alicante, Secretariado de Publicaciones, 1997, p. 167.
- [95] J.B. Donnet, R.C. Bansal, M.J. Wang, Carbon Black Science and Technology, 2nd ed., Marcel Dekker, New York, 1993.
- [96] J.P. Zheng, T.R. Jow, J. Power Sources 62 (1996) 155.
- [97] T. Osaka, X. Liu, M. Nojima, J. Power Sources 74 (1998) 122.
- [98] F. Beck, M. Dolata, E. Grivei, N. Probst, J. Appl. Electrochem. 31 (2001) 845.
- [99] R. Richner, S. Müller, A. Wokaun, Carbon 40 (2002) 307.
- [100] R.W. Pekala, J. Mater. Sci. 24 (1989) 3221.
- [101] H. Pröbstle, M. Wiener, J. Fricke, J. Porous Mater. 10 (2003) 213.
- [102] U. Fischer, R. Saliger, V. Bock, R. Petricevic, J. Fricke, J. Porous Mater. 4 (1997) 281.
- [103] C. Schmitt, H. Pröbstle, J. Fricke, J. Non-Cryst. Solids 285 (2001) 277.
- [104] H. Pröbstle, C. Schmitt, J. Fricke, J. Power Sources 105 (2002) 189.
- [105] R. Petricevic, M. Gloor, J. Fricke, Carbon 39 (2001) 857.
- [106] S. Escribano, S. Berthon, J.L. Ginoux, P. Achard, Extended Abstracts: Eurocarbon'98, Strasbourg, France, 1998, pp. 841–842.
- [107] W. Li, G. Reichenauer, J. Fricke, Carbon 40 (2002) 2955.
- [108] R. Saliger, G. Reichenauer, J. Fricke, in: K.K. Unger, et al. (Eds.), Characterization of Porous Solids V, Elsevier, 2000, p. 381.
- [109] S.H. Yoon, Y. Korai, I. Mochida, H. Marsh, F. Rodriguez-Reinoso (Eds.), Sciences of Carbon Materials, Universidad de Alicante, 2000, p. 287.
- [110] A. Nishino, Proceedings of the 183rd Meeting of the Electrochemical Society, vol. 93-23, Honolulu, Hawaii, 1993, p. 1.
- [111] A. Braun, M. Bärtsch, B. Schnyder, R. Kötz, O. Haas, H.-G. Haubold, G. Goerigk, J. Non-Cryst. Solids 260 (1999) 1.
- [112] A. Oya, H. Marsh, E.A. Heintz, F. Rodriguez-Reinoso (Eds.), Introduction to Carbon Technologies, Universidad de Alacante, 1997, p. 561.
- [113] G.M. Jenkins, K. Kawamura, Polymeric Carbons–Carbon Fibre, Glass and Char, Cambridge University Press, Cambridge, 1976.
- [114] M.G. Sullivan, M. Bärtsch, R. Kötz, O. Haas, Proceedings of the Electrochemical Society, vol. 96-25, The Electrochemical Society, Pennington, NJ, 1996, p. 192.
- [115] A. Braun, M. Bärtsch, B. Schnyder, R. Kötz, O. Haas, A. Wokaun, Carbon 40 (2002) 375.
- [116] A. Braun, M. Bärtsch, O. Merlo, B. Schnyder, B. Schaffner, R. Kötz, O. Haas, A. Wokaun, Carbon 41 (2003) 759.
- [117] D. Alliata, P. Häring, O. Haas, R. Kötz, H. Siegenthaler, Electrochem. Solid-State Lett. 2 (1999) 33.
- [118] N.M. Rodriguez, J. Mater. Res. 8 (1993) 3233.
- [119] B. McEnaney, Prace Naukowe Instytutu Chemii i Technologii Nafty i Wegla. Politechniki Wroclawskiej, Konferencje 57 (2002) 10.
- [120] K.H. An, K.K. Jeon, J.K. Heo, S.C. Lim, D.J. Bae, Y.H. Lee, J. Electrochem. Soc. 149 (2002) A1058–A1062.
- [121] Y.H. Lee, K.H. An, S.C. Lim, W.S. Kim, H.J. Jeong, C.-H. Doh, S.-I. Moon, New Diamond Frontier Carbon Technol. 12 (2002) 209.
- [122] K.H. An, W.S. Kim, Y.S. Park, J.-M. Moon, D.J. Bae, S.C. Lim, Y.S. Lee, Y.H. Lee, Adv. Funct. Mater. 11 (2001) 387.



- [123] E. Frackowiak, K. Jurewicz, S. Delpeux, F. Béguin, L.M. Liz-Marzán, M. Giersig (Eds.), *Low-dimensional Systems: Preparation, and Some Applications*, Kluwer Academic Publishers, 2003, p. 305.
- [124] E. Frackowiak, K. Jurewicz, K. Szostak, S. Delpeux, F. Béguin, *Fuel Process. Technol.* 77/78 (2002) 213.
- [125] E. Frackowiak, S. Delpeux, K. Jurewicz, K. Szostak, D. Cazorla-Amoros, F. Béguin, *Chem. Phys. Lett.* 361 (2002) 35.
- [126] E. Frackowiak, F. Béguin, *Carbon* 39 (2001) 937.
- [127] F. Frackowiak, K. Metenier, V. Bertagna, F. Béguin, *Appl. Phys. Lett.* 77 (2000) 2421.
- [128] C. Niu, E.K. Sichel, R. Hoch, D. Moy, H. Tennent, *Appl. Phys. Lett.* 70 (1997) 1480.
- [129] Q. Jiang, M.Z. Qu, G.M. Zhou, B.L. Zhang, Z.L. Yu, *Mater. Lett.* 57 (2002) 988.
- [130] K.H. An, W.S. Kim, Y.S. Park, Y.C. Choi, S.M. Lee, D.C. Chung, D.J. Bae, S.C. Lim, Y.H. Lee, *Adv. Mater.* 13 (2001) 497.
- [131] M. Hughes, G.Z. Chen, M.S.P. Shaffer, D.J. Fray, A.H. Windle, *Chem. Mater.* 14 (2002) 1610.
- [132] J.H. Chen, W.Z. Li, D.Z. Wang, S.X. Yang, J.G. Wen, Z.F. Ren, *Carbon* 40 (2002) 1193.
- [133] Ch. Emmenegger, P. Mauron, A. Züttel, Ch. Nützenadel, A. Schneuwly, R. Gally, L. Schlapbach, *Appl. Surf. Sci.* 162/163 (2000) 452.
- [134] J.H. Chen, W.Z. Li, Z.P. Huang, D.Z. Wang, S.X. Yang, J.G. Wen, Z.F. Ren, *Proceedings of the 197th Meeting of the Electrochemical Society, Toronto, Canada, 2000.*
- [135] H. Tamai, K. Masayuki, M. Morita, H. Yasada, *Electrochem. Solid State Lett.* 6 (2003) A214–A217.



本文献由“学霸图书馆-文献云下载”收集自网络，仅供学习交流使用。

学霸图书馆（www.xuebalib.com）是一个“整合众多图书馆数据库资源，提供一站式文献检索和下载服务”的24小时在线不限IP图书馆。

图书馆致力于便利、促进学习与科研，提供最强文献下载服务。

#### 图书馆导航：

[图书馆首页](#)    [文献云下载](#)    [图书馆入口](#)    [外文数据库大全](#)    [疑难文献辅助工具](#)